The effect of electrospark nickel interlayer thickness on the characteristics of Niobium to 410 stainless steel dissimilar laser welding

Baghjari, Seyed Hamzeh; Malek Ghaini, Farshid; Previtali, Barbara; Gokhan Demir, Ali; Shahverdi, Hamid Reza; Mapelli, Carlo; Barella, Silvia

The effect of electrospark nickel interlayer thickness on the characteristics of Niobium to 410 stainless steel dissimilar laser welding

Seyed Hamzeh Baghjari [a], Farshid Malek Ghaini [a], Barbara Previtali [b], Ali Gokhan Demir [b], Hamid Reza Shahverdi [a], Carlo Mapelli [b], Silvia Barella [b]

[a] Department of Materials Engineering, Tarbiat Modares University, Tehran, Iran
[b] Dipartimento di Meccanica, Politecnico di Milano, Via La Massa 34, 20156 Milan, Italy

Abstract

Dissimilar welding of Niobium to 410 stainless steel has important engineering applications. An inter-layer should be used for avoiding or reducing formation of brittle intermetallic phases in weld. In this research the effect of gradual addition of ESD interlayer on the chemical composition, microstructure and mechanical properties of Nb to 410 stainless steel dissimilar laser welding is investigated. The Nb plate with the ESD interlayer thickness equivalent to about 25%, 50%, and 100% of base plate thicknesses on its edge (produced by novel electrospark deposition process) was laser welded to 410 stainless steel by pulsed Nd:YAG laser. The welds were then subjected to metallographic, X-ray diffraction and mechanical tests. Results showed that with an increase in ESD interlayer thickness, the weldability increased due to reduction of brittle and -Laves intermetallic phases in the fusion zone. Tensile test results of dissimilar Nb to 410 stainless steel weld, showed that the chemical composition of the dissimilar weld zone deter-mines the mechanical strength of the joint. Furthermore, in order to reach high mechanical strengths, contact of the weld pool and its solidification on the Nb also has to be avoided due to formation of brittle -Laves phase.

Introduction

The high quality dissimilar junction between Niobium alloys and stainless steel have some applications in aerospace industries like turbojet engines which are subjected to high temperature and stress [1]. The main difficulty in joining Niobium to stainless steel using fusion is their large differences in thermo-physical properties and the formation of brittle intermetallic compounds (like -Fe_2 Nb and -Fe_7 Nb_6 with hardness of about 1000 HV) which degrade the mechanical properties of the dissimilar weld [2,3]. To obtain an acceptable mechanical strength for Nb to stainless steel joint, an interlayer should be used. However, using an interlayer in the form of a strip has its own technical limitations [4].

Electrospark deposition (ESD) is a low heat input deposition process that uses short-duration, high-current electrical pulses to weld a consumable electrode material to a metallic substrate [5]. Vishwakarma et al. [6] and Ebrahimnia et al. [7,8] used ESD for repairing IN718 and IN738LC gas turbine blade materials, Which are both considered as alloys generally difficult to be welded. The formation of brittle intermetallic compounds would be the main problem in Niobium to 410 steel welding. However, Baghjari et al.

[3] incorporated electrospark interlayer for dissimilar laser weld-ing of Nb to 410 steel and reported that, very low heat input and also dilution with the respective substrate, make ESD desirable for welding incompatible dissimilar joints Also Gould [9] used electro-spark deposition for dissimilar welding of refractory metals to cast Ni-based superalloy, with a Hastelloy X filler metal. He reported formation of no brittle intermetallic compounds at the interface.

The Laves phase is an intermetallic compound with a hexagonal crystal structure and A_2 B stoichiometry. In laves phase "A" indi-cates elements such as Ni, Fe and Cr, and "B" indicates elements such as Nb, Ti and Mo [10]. Laves phase exists in the simple Fe-Nb binary phase diagram over a composition range of 38–50 wt.% Nb. The formation of the Laves phase is because of the micro segregation of alloying elements in non-equilibrium solidification conditions, mostly for high atomic diameter elements like Nb, Mo and Ti [11].

Rather than increasing Ni, the addition of Fe to Ni-Nb alloys increases Fe content of the austenite matrix and hence pro-motes the formation of more /Laves. Also Fe, Cr, and Si increase the segregation tendency of Nb and promote Laves at the expense of -Ni$_3$ Nb [12,13,15].

In our previous research [3], we focused on the characteriza-tion of electrospark nickel interlayer and showed that using this interlayer is useful in improving the dissimilar Nb to 410 steel weldability. However, in the present work the main goal is to study the effect of gradual addition of ESD interlayer on Nb to 410 steel dissimilar laser welding, which is deposited by the elec-trospark deposition process (ESD). The complex microstructure evolution across the dissimilar laser welds as well as the mechan-ical properties of the joints are investigated. With the addition of ESD interlayer in weld, dilution of Nb base metal is reduced, which has effects on the amount of intermetallic compounds formation.

Overall, in the present study, the amount of acceptable dilution of the Nb and ESD interlayer alloying elements in the final laser weld metal to achieve the weld with appropriate mechanical proper-ties, are determined. It is envisaged that the output of this research would confer intriguing potential in technological advancement of the very field.

Experimental procedure

The pure Nb and 410 stainless steel plates with

1 mm × 100 mm × 10 mm dimension were prepared by wire cut. A Ni based interlayer, Alloy 82, in the shape of a rod with 2 mm diameter used as filler metal in ESD process. The chemical composition of base metals and filler metal are shown in Table 1.

In the first stage, a groove was made on one side of the Nb plate by grinding, and then this groove was filled with ESD process using an Alloy 82 filler with 2 mm thickness. Then with grinding on the back of the first side, another similar groove was made on the sec-ond side to obtain a thicker interlayer. The schematic of preparing ESD interlayer on Nb plate edge, can be seen in Fig. 1. Electrospark interlayer deposited with ESD machine was developed in Tarbiat Modares University and with the following parameters: voltage of 120 V, duty cycle of 3%, frequency of 204 Hz and capacitance of 480 microfarad. The electrode was oriented at angle of 30–45∘ to the substrate and was rotating at the speed of 2000 RPM during depo-sition. The shielding argon gas was delivered to the work piece at 20 ml/min flow rate. After the Alloy 82 interlayer was deposited on both sides of the Nb plate, it was wire cut from the middle to form two Nb plates which were built up of an ESD interlayer over their edges. With this method, interlayer thicknesses of about 25%, 50%, and 100% of base plate thickness were obtained; see Fig. 2 stage 1, through (d). Then the Nb plates with different thicknesses of Alloy 82 ESD interlayer, were laser welded to 410 stainless steel. Fig. 2 shows schematics of the configuration (stage 2). A pulsed Nd:YAG laser welding machine with a maximum mean laser power of 120 W was used for welding. Pure argon gas with 20 ml/min flow rate was used for shielding. Full penetration welds were obtained using a laser spot diameter of 0.3 mm, pulse frequency of 13 Hz, pulse duration of 7 ms, energy per pulse of 7 J and welding speed of 200 mm/min, which were found to be an optimum set of process parameters through trials. In this article the 0.25, 0.5 and 1 mm thickness samples mean dissimilar welds with 0.25, 0.5 and 1 mm interlayer thickness.

Samples were cut in cross sections for metallographic study. Glyceregia (30 ml H$_2$ O–60 ml HCl–20 ml HNO$_3$) was used for etching the dissimilar laser weld samples. Microstructural inves-tigations were performed by Hitachi SU-70 TFEG scanning electron microscope equipped with Thermo Scientific EDS detector. Sec-ondary and backscattered electron imagining micrographs and EDS analyses were taken with an acceleration voltage of 15 kV. X-ray diffraction (XRD) analysis was performed on weld zone for identi-fication of phases

in the fusion zone. For this purpose, two base metals of the weld were cut out and the bulk weld metal with approximately 0.5 mm × 1 mm × 10 mm dimensions was analyzed by X'Pert Pro MPD machine. This XRD equipment due to high sensitivity and resolution can identify the phases in such narrow sample. The microhardness of weld metal was measured using a Vickers micro indentation device at 100 g load and 15 s loading time. Tensile tests which were prepared according to ASTM: E8/8 M were performed on weld samples. This test was performed using a CMT6305-300 KN electro-mechanical universal testing machine at room temperature. The strain rate was set at 10^{-3} S^{-1} . Each tension test was repeated two times.

Results and discussion

Fig. 2 shows the cross sections of Nb to 410 stainless steel dis-similar laser welds made with various nominal thicknesses of ESD interlayer. In dissimilar laser weld without interlayer, the weld was completely broken from 410 steel side, while in samples with 0.25 mm interlayer thickness, transverse cracks were observed in the weld zone (Fig. 3a and b). Furthermore, no cracks were observed with the 0.5 and 1 mm interlayer thickness welds. It is necessary to point out that the formation of brittle -Laves and phases causes brittleness in the weld zone. Moreover, thermal stresses which originate from solidification, are one of the main reasons of track in the weld zone. That is to say, the combination of these two phenomena in the weld zone, leads to cracking in the dissimilar weld metal and further illustrates different results obtained with different interlayer thicknesses. However, increasing Ni content of the weld metal leads to suppression of -$Fe_7 Nb_6$ phase formation and decreasing the brittle -Laves phases content in weld zone.

The average (bulk) chemical composition and elemental distri-bution profile of welds as measured by EDS are shown in Table 2 and Fig. 4. As expected, an increase in the thickness of ESD interlayer, the content of Ni element is also increased and Nb concentration is decreased. The presence of base metals and interlayer dilution in Table 3 confirm increasing the thickness of ESD interlayer, reduce the Nb dilution from 70% to 5%.

By using the ternary phase diagram of Fe-Nb-Ni isothermal sec-tion at 1200 ◦ C which is shown in Fig. 5, and locating the chemical compositions of welds on the ternary phase diagram, a predic-tion can be made about the possible phases comprising the weld microstructure. Due to the fast cooling during laser welding, imme-diately after solidification of weld pool, the temperature falls down to room temperature and there is not enough time for diffusion. Therefore microstructure of laser weld will be very similar and can be predicted by the isothermal section of Fe-Nb-Ni diagram at high temperature (1200 ◦ C). On the other hand the X-ray diffraction analysis of the bulk of the weld metals as shown in Fig. 6 is an evidence of the phases actually formed with the fast cooling rates involved in laser weld-ing. It can be seen that the result of X-ray diffraction analysis is in confirmation with the phases predicted in Table 2 in this occa-sion. The results indicate that, without using the ESD interlayer, the weld zone consists mainly of -$Fe_7 Nb_6$, -$Fe_2 Nb$ and Nb phases (Fig. 6a). With an increase of ESD interlayer thickness to 0.25 mm, -$Fe_2 Nb$ diffraction peaks became stronger and diffraction peaks are appeared. With further increase in ESD interlayer thickness to 0.5 and 1 mm, the diffraction peaks dominate the pattern. The Ni-rich weld metal promotes the formation of phase since it is an austenite phase former. The formation of -$Fe_2 Nb$ phases is partly suppressed due to the decreasing of the Nb and Fe contents of the weld (Table 2 and Fig. 4).

Fig. 7 shows the Nb to 410 stainless steel dissimilar laser weld without ESD interlayer. As can be seen, the appearance of the etched macro section shows that the weld metal is almost divided into two zones with different Nb and Fe contents (see Fig. 7a). This is indica-tive of incomplete mixing, possibly due to significant differences in the melting point and other physical properties of the two base metals. [14]. The phases identified in the two zones were numbered as in Fig. 7b and c and their chemical compositions were determined by EDS as shown in Table 4. Identification of these phases can be facilitated by referring to the Fe-Nb binary phase diagram and X-ray diffraction results (Fig. 6a). Line A in Fig. 8 which is the Nb-Fe binary phase diagram, represents the chemical composition of zone A. The main phase in zone A is expected to be dendritic Nb with the -$Fe_7 Nb_6$ +Nb eutectic dispersed around it, which are the prod-ucts of the eutectic reaction (L = -$Fe_7 Nb_6$

+Nb). The bright phase in Fig. 7d is rich in Nb. Line B represents the composition of zone B. Compared to zone A, zone B has less Nb content. Microstructure of this zone is mainly composed of -Fe_7Nb_6 intermetallic phase with eutectic -Fe_7Nb_6 + Nb structure dispersed around it.

Fig. 9 shows the cross section and microstructure of Niobium to 410 stainless steel dissimilar laser weld with a 0.25 mm nominal thickness ESD interlayer. Due to high Nb dilution and incomplete mixing, different areas were observed in weld zone. The EDS analy-sis revealed that in different areas of the fusion zone, the Nb and Fe contents are different. Two areas of the fusion zone identified as C and D were chosen to investigate the microstructures (Fig. 9a). The main phase in zone C is composed of -Laves phase (light) in addi-tion to some -Laves + eutectic phase (Fig. 9b). The -Laves phase is in the form of $(Fe, Ni, Cr)_2$ Nb. The microstructure of zone D is a mixture of -Laves and more -Laves + eutectic dispersed around it due to lower Nb content (Fig. 9c). Higher magnification of the eutectic phase, which its formation could be explained by the fol-lowing local invariant reactions (L = -Laves +), is shown in Fig. 9d. Due to the eutectic reaction, the microstructure exhibits a lamellar morphology. The formation of -Laves phase and -Laves + eutec-tic in the weld zone can be confirmed by the chemical composition of different phases in Fig. 9b, c and according to Fe-Nb-Ni ternary phase diagram (Table 4). The cross section and microstructure of Nb to 410 stainless steel dissimilar laser weld with a 0.5 mm nominal thickness ESD interlayer are shown in Fig. 10 and chemical analysis of the points obtained by EDS are shown in Table 4. Microstructure of weld in zone E consists of matrix with -Laves + eutectic phase around it, which is proved by Fe-Nb-Ni ternary phase diagram and its chemical composition of different phases is represented in Table 4. Diffraction patterns in Fig. 6c confirm the formation of -Laves phase which is a hexagonally close packed phase in the form of $(Fe, Ni, Cr)_2$ Nb. As shown in Table 4, the addition of Ni to weld decreases Fe and Nb content which is well known to promote phase at the expense of the -Laves phase [12,13]. Thus, increasing ESD inter- layer thickness from 0.25 to 0.5 mm, changes the microstructure from -Laves matrix with -Laves + eutectic around it to matrix with -Laves + eutectic around it. This would lead to an improve-ment in the wealability of the joint and ultimately prevention of cracking.
Fig. 10d shows the interface of weld/Nb (zone F in Fig. 10a) at a higher magnification. According to EDS analysis, there is a layer between the dendritic part of the fusion zone and solid Nb base metal. The chemical composition of this layer (location 11) in Fig. 10d represented in Table 4, shows that this layer has thick-ness of about 5 m and is expected to be -Laves. This interface layer is generated by diffusion of the liquid Fe, Ni and Cr atom-ics into solid Nb base metal. In fact, the competing diffusion flows of weld pool elements penetrate into the Nb base metal forming the interface with different phase composition. This layer has very high hardness and consists of micro cracks. Therefore this layer is the weakest area of weld zone and reduces the strength of joint. The formation of intermetallic layer in interface of dissimilar laser welding was previously observed by Tomashchuk et al. [15] and Chu et al. [16] in Titanium to steel dissimilar welding. Diffusion of molten steel toward solid Niobium and formation of intermetallic layer was observed by Budkin et al. [2] in dissimilar weld brazing of Niobium and steel using electron beam. Torkamany et al. [17] found out Ti atoms in the molten pool can diffuse into the solid Niobium to form a thin layer of Ti–Nb with a melting temperature less than pure Niobium in dissimilar pulsed laser welding of Niobium and Ti–6Al–4 V.

The cross section and microstructure of Nb to 410 stainless steel dissimilar laser weld with the 1 mm nominal thickness ESD inter-layer is shown in Fig. 11 with the corresponding chemical analysis in Table 4. The microstructure of the weld metal is mainly phase with a dendritic morphology where -Laves has formed a contin-uous network in the interdendritic regions. The -Laves phase is a hexagonally close packed phase in the form of $(Ni, Fe, Cr)_2$ Nb. EDS analysis indicates the formation of and -Laves phases in weld zone. However, X-ray diffraction only identified the phase (Fig. 6d). This can be due to the fact that in weld with 1 mm ESD interlayer thickness, some part of nickel based ESD interlayer remained in XRD sample. The amount of laves phase in ESD inter-layer is very low compare to weld metal and XRD pattern of ESD interlayer is very similar to weld metal which is nickel based alloy too. Thus at this condition the amount of laves phase

which mainly formed in weld, in sample examined by XRD was below 5% and could not be detected. But from microstructure images and EDS analyses we know laves phase is formed in weld metal and its con-tent is more than 5%. This can be the result of the decreasing in Nb and Fe contents in the weld which is expected to decrease the percentage of -Laves even below the detection limit of the XRD apparatus.

Fig. 11c shows the high magnification image of the interface of the fusion zone of the dissimilar weld at the location where it solidified over the ESD interlayer (zone H in Fig. 11a). As can be seen the interface morphology is quite different from that when Nb directly is in contact with the fusion zone without interlayer (Fig. 10d). Furthermore, Fig. 11d shows the interface of the fusion zone at the location where it solidified over the Nb base (zone L in Fig. 11a). Again according to EDS analysis there is a layer between the dendritic fusion zone and the Nb base metal. The chemical com-position of this layer in Table 4 matches with -Laves phase which was generated by diffusion of the liquid Fe, Ni and Cr atomics into solid Nb base metal [19]. Although this layer is expected to be brit-tle, the tensile strength of the joint is not apparently compromised, because in this case it has formed only on a very limited area of the joint. This findings point to the main advantage of using ESD to produce an interlayer on Nb (instead of using a strip of Nickel). With ESD interlayer, there is no need for the laser beam to melt any Nb in order to achieve a metallurgical bond. Thus, the formation of the brittle intermetallic layer between Nb and the laser weld pool can be avoided.

Fig. 12 shows microhardness profiles of dissimilar laser weld joints. The ESD interlayer thickness has a great effect on the fusion zone hardness. With increasing the interlayer thickness the hard-ness of dissimilar weld decreases dramatically. Without using the ESD interlayer (0 mm thick) the average hardness value of weld zone was 709 HV. According to X-ray diffraction analysis, appar-ently, in weld with 0 and 0.25 mm interlayer thicknesses, the formation of -Fe_2 Nb Laves and -Fe_7 Nb_6 phases in weld zone is the main reason for the high hardness value. But with using 0.5 and 1 mm interlayer thickness due to the reduction of such brittle phases, the average hardness value reduced to 312 HV and 259 HV, respectively.

Due to the formation of transverse cracks in Nb to 410 stainless steel dissimilar laser weld without and with only 0.25 mm nomi-nal ESD interlayer thickness, tensile strength of these welds were considered meaningless to be evaluated. However, with no ESD interlayer, the joint fracture occurred in the 410/Weld interface once a tensile load was applied (almost zero strength). Tensile tests results of Nb to 410 stainless steel dissimilar laser weld with 0.5 mm thickness ESD interlayer in Fig. 13 (two on each), were shown joint strength is significantly low (only 70 MPa). This observation is in spite of decreasing brittle intermetallic phases and the relatively lower average hardness of the fusion zone [18]. It is believed that the joint strength in this case is deteriorated by the brittle weld/Nb interfacial intermetallic such as -Laves phase as can be seen in Fig. 10a (zone F). In Fig. 14 the cross section of fracture path in weld/Nb interface and fracture surface are shown. When Nb comes into contact with the Fe, Ni and Cr contaminated molten laser weld pool, a brittle -Laves phase layer, with less than 5 m width will form on weld/Nb interface in solidification. The brittle fracture surface of 0.5 mm interlayer thickness weld confirms that the fracture path is prorogated in brittle -Laves phase layer (Fig. 14b). However, in the case of the dissimilar weld with 1 mm ESD interlayer thickness, the ultimate strength was 285 MPa and the failure was located in Nb base metal away from the weld fusion line (Fig. 13). This indicates the high strength of weld metal and strong metallurgical bonding between Nb and the ESD interlayer and the weld zone. By increasing the ESD interlayer thickness to 1 mm, the formation of brittle -Laves phases within the weld and weld/Nb interface is significantly reduced (only area L in Fig. 12a). The above observations show that for a successful dissimilar weld, in additionof decreasing intermetallic phases in weld zone, almost no contacts between the weld pool and the Nb base metal is allowed. By placing the interlayer with ESD process, there is no need for the laser beam to melt any Nb in order to achieve a metallurgical bond. By using a thick enough interlayer (in this case about 1 mm thick), the contact of weld pool and Nb base is limited and this technique significantly improves the strength of the dissimilar weld.

Conclusions

The characterization of different phases and mechanical prop-erties in Nb to 410 stainless steel dissimilar laser welding, with various thicknesses of ESD interlayer was studied and conclusions were summarized as following:

1. With an increase in ESD interlayer thickness, the weldability increased due to reduction of the amount of brittle -Fe$_7$Nb$_6$ and -Laves phases in the fusion zone.

2. Without using Ni interlayer the main phases in weld zone are Nb, -Fe$_7$Nb$_6$ and -Fe$_2$Nb. Increasing Ni interlayer to 0.5 mm thick, results in changing the microstructure from -Laves matrix with -Laves + eutectic around it to matrix with -Laves + eutec-tic around it.

3. The hardness of Nb to 410 stainless steel weld with 0 and 0.25 mm thick interlayer are significantly higher compared to that with 0.5 and 1 mm thick Ni interlayer confirming the role of hard -Laves phase.

Tensile test showed that it is not only the chemical composi-tion of the final fusion zone which determines the mechanical strength of the dissimilar weld, but also any direct contact of the

Acknowledgement

References

[1]   Mastanaiah P, Madhusudhan Reddyb G, Satya Prasadb K, Murthya CVS. An investigation on microstructures and mechanical properties of explosive cladded C103 niobium alloy over C263 nimonic alloy. J Mater Process Technol 2014;214:2316–24.

[2]   Budkin Yu V, Erofeev VA. A physico–mathematical model of the formation of intermetallic compounds in weld brazing of refractory metals to steel. Weld Inter 2011;25(8):633–7.

[3]   Ng Edwin CH, Mokm SH, Man HC. Effect of Ta interlayer on laser welding of NiTi to AISI 316L stainless steel. J Mater Process Technol 2011;226:69–77.

[4]   Baghjari SH, Malek Ghaini F, Shahverdi HR, Mapelli C, Barella S, Ripamonti D. Laser welding of niobium to 410 stainless steel with a nickel interlayer pro-duced by electro spark deposition. Mater Des 2016;107:108–16.

[5]   Baghjari SH, Malek Ghaini F, Shahverdi HR, Ebrahimnia M, Mapelli C, Barella S. Characteristics of electrospark deposition of a nickel-based alloy on 410 stain-less steel for purpose of facilitating dissimilar metal welding by laser. Inter J Adv Manuf Technol 2016;87:2821–8.

[6]   Vishwakarma KR, Ojo OA, Richards NL. Nano-size solidification micro con-stituents in electro-spark deposited Ni-base superalloy. Philos Mag Lett 2015;95:30–6.

[7]   Ebrahimnia M, Malek Ghaini F, Xie YJ, Shahverdi HR. Developing new microstructure through laser melting of electrospark layer of precipitation hardened nickel based superalloy. Sci Technol Weld Join 2016;21(7):570–7.

[8]   Ebrahimnia M, Ghaini FM, Shahverdi HR. Hot cracking in pulsed laser process-ing of a nickel based superalloy built up by electrospark deposition. Sci Technol Weld Join 2014;19(1):25–9.

[9]   Gould J. Application of electro-spark deposition as a joining technology. Weld J 2011;90:191s–7s.

[10]   DuPont JN, Lippold JC, Kiser SD. Welding metallurgy an weld ability of nickel-base alloys. New Jersey: John Wiley & Sons Inc; 2009.

[11]   Voß S, Palm M, Stein F, Raabe D. Phase equilibrium in the Fe-Nb system. J Phase Equilib Diff 2011;32(2):97–104.

[12]   Jacob A, Schmetterera C, Khvanc A, Kondratievc A, Ivanovc D, Hallstedtd B. Liq-uidus projection and thermodynamic modeling of the Cr-Fe-Nb ternary system. Comp Coupl Phase Diag Thermochem 2016;54:1–15.

[13]   Mathon M, Connétable D, Sundman B, Lacaze J. Calphad-type assessment of the Fe-Nb-Ni ternary system. Comp Coupl Phase Diag Thermochem 2009;33:136–61.

[14]   Torkamany MJ, Malek Ghaini F, Poursalehi R. Dissimilar pulsed Nd:YAG laser welding of pure niobium to Ti–6Al–4 V. Mater Des 2014;53:915–20.

[15]   Tomashchuk I, Sallamand P, Belyavina N, Pilloz M. Evolution of microstructures and mechanical properties during dissimilar electron beam welding of titanium alloy to stainless steel via copper interlayer. Mater Sci Eng A 2013;585:114–22.

[16]   Chu Q, Zhanga M, Lia J, Fana Q, Xiea W, Bib Z. Joining of CP-Ti/Q345 sheets by Cu-based filler metal and effect on interface. J Mater Process Technol 2015;225:67–76.

[17]   Torkamany MJ, Malek Ghaini F, Poursalehi R. An insight to the mechanism of weld penetration in dissimilar pulsed laser welding of niobium and Ti–6Al–4 V. Opt Laser Technol 2016;79:100–7.

[18]   Deepan Bharathi Kannan T, Sathiya P, Ramesh T. Experimental investigation and characterization of laser welded NiTinol shape memory alloys. J Manuf Process 2017;25:253–61.

[19]   Satpathya MP, Kumar Sahoob S. Mechanical performance and metallurgical characterization of ultrasonically welded dissimilar joints. J Manuf Process 2017;25:443–51.

Table 1

Chemical composition of base metals and filler metal.

Nb wt%	Ti wt%	S wt%	P wt%	Ni wt%	Cr wt%	Mn wt%	Fe wt%	C wt%	Alloy
0.0	0.0	0.02	0.02	0.20	12.30	1.00	Balance	0.08	AISI 410
2.74	0.4	0.01	0.03	Balance	21.87	3.14	0.36	0.05	Alloy 82
99.99	0	0	0	0	0	0	0	0	Niobium

Table 2

Average EDS chemical analysis of dissimilar laser weld of Nb to 410 stainless steel with different nominal ESD interlayer thicknesses

Ni interlayer Thickness		Ti	Cr	Mn	Fe	Ni	Nb	EDS phases + Phase diagram
0 mm	wt%	0	3.7	0.11	28.8	0.10	67.40	-Fe7 Nb6 + Nb
	at%	0	5.41	0.15	39.19	0.13	55.12	
0.25 mm	wt%	0.06	10.8	0.9	52.7	12.84	22.7	-(Fe, Cr, Ni)2 Nb +
	at%	0.08	12.73	1.0	57.82	13.4	14.97	
0.5 mm	wt%	0.10	13.7	0.8	58.4	18.1	8.9	+ -(Fe, Cr, Ni)2 Nb
	at%	0.12	15.23	0.54	60.45	17.82	5.54	
1 mm	wt%	0.19	18.27	2.54	16.72	54.62	7.66	+ -(Fe, Cr, Ni)2 Nb
	at%	0.23	20.5	2.7	17.47	54.29	4.81	

Table 3

Dilution percent of two base metals and ESD interlayer in dissimilar laser weld of Nb to 410 stainless steel with different nominal ESD interlayer thicknesses

Ni interlayer Thickness	410 steel	Nb	Nickel 82 interlayer
0 mm	30	70	0
0.25 mm	60	20	20
0.5 mm	65	10	25
1 mm	20	5	75

Table 4

Chemical compositions (at.%) at each location.

Spectrum	Cr	Fe	Ni	Nb	Potential phases
1	1.7	11.85	0	86.45	Nb
2	3.49	24.78	0	71.73	Nb
3	5.14	39.23	0	55.63	-Fe7 Nb6 + Nb
4	4.53	34.03	0	61.44	-Fe7 Nb6 + Nb
5	8.93	49.64	0	41.43	-Fe7 Nb6
6	11.46	57.77	9.84	20.93	-(Fe, Ni, Cr)2 Nb
7	1.91	68.72	8.50	20.88	(-Fe2 Nb +) eutectic
8	12.37	53.95	15.15	18.53	-(Fe, Ni, Cr)2 Nb
9	15.48	65.86	14.49	4.18	
10	13.26	59.41	13.00	14.33	(-(Fe, Ni, Cr)2 Nb +) eutectic
11	13.77	59.74	12.79	13.7	(-(Fe, Ni, Cr)2 Nb +) eutectic
12	20.39	20.11	53.45	6.04	
13	18.69	12.33	54.60	14.38	(-(Fe, Ni, Cr)2 Nb +) eutectic
14	17.57	11.87	57.04	13.51	(-(Fe, Ni, Cr)2 Nb +) eutectic
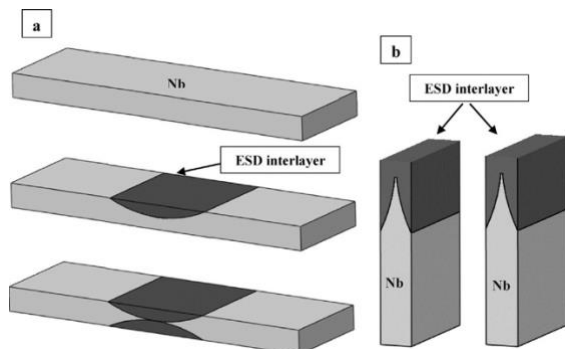
Fig. 1. Schematic of Nb plate with ESD interlayer, a- before cutting, b- after cutting.
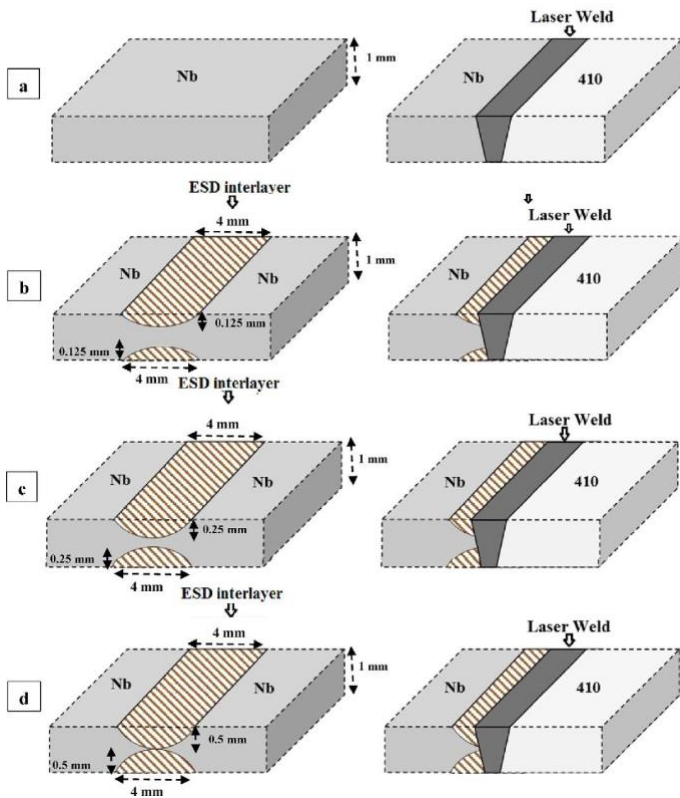
Fig. 2. Schematic of laser welding Nb plate with different nominal ESD interlayer thicknesses to 410 stainless steel. a- No interlayer, b- 0.25 mm thick, c-0.5 mm thick, d-1 mm thick.
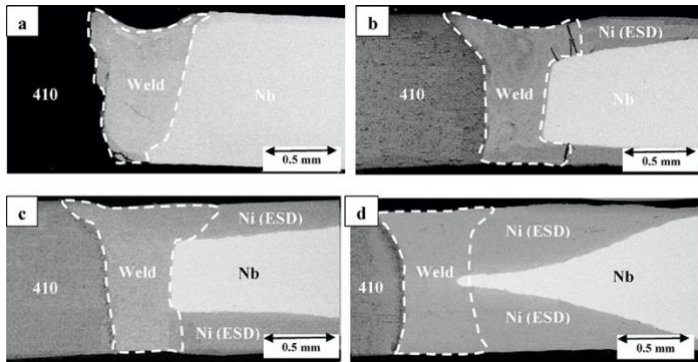

Fig. 3. Cross section of dissimilar laser weld of Nb to 410 steel with different nominal ESD interlayer thicknesses, a- No interlayer (cracked), b-0.25 mm thick (cracked), c-0.5 mm thick, d-1 mm thick.
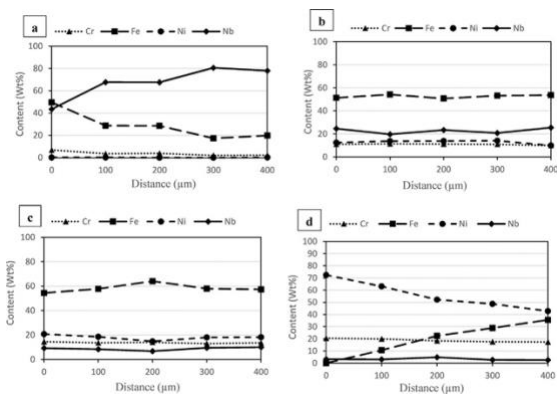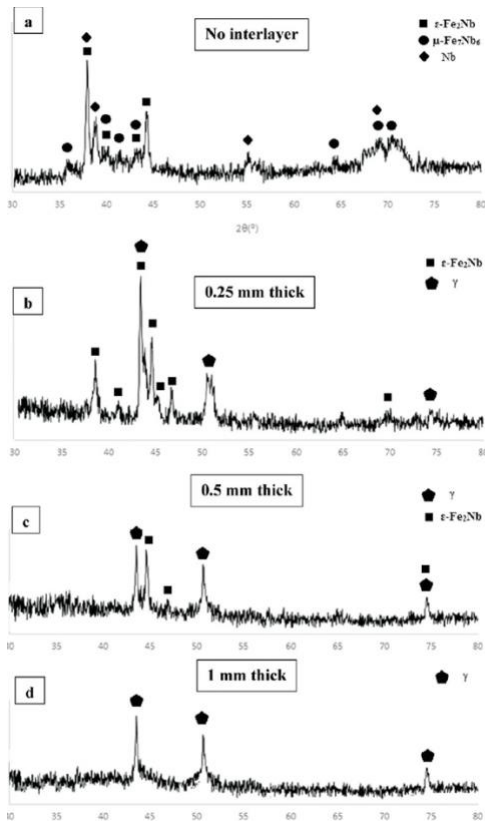

Fig. 4. Elemental distribution profile of dissimilar laser weld of Nb to 410 steel with different ESD interlayer, a- No interlayer, b- 0.25 mm thick, c-0.5 mm thick, d-1 mm thick.
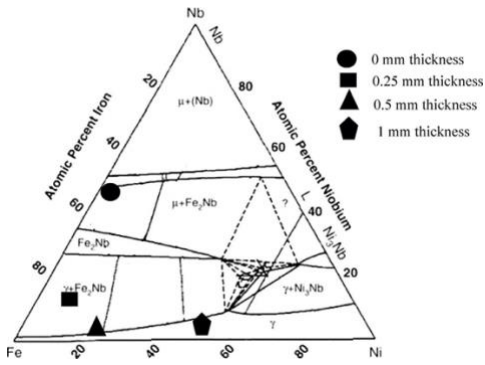
Fig. 5. Fe-Nb-Ni isothermal section at 1200C∘ , chemical composition of weld metal with different nominal thicknesses of ESD interlayer (0, 0.25, 0.5 and 1 mm) are superimposed [13].

Fig. 6. X-ray diffraction patterns of dissimilar laser weld of Nb to 410 steel with different nominal ESD interlayer thicknesses, a- No interlayer, b- 0.25 mm thick, c-0.5 mm thick, d–1 mm thick.
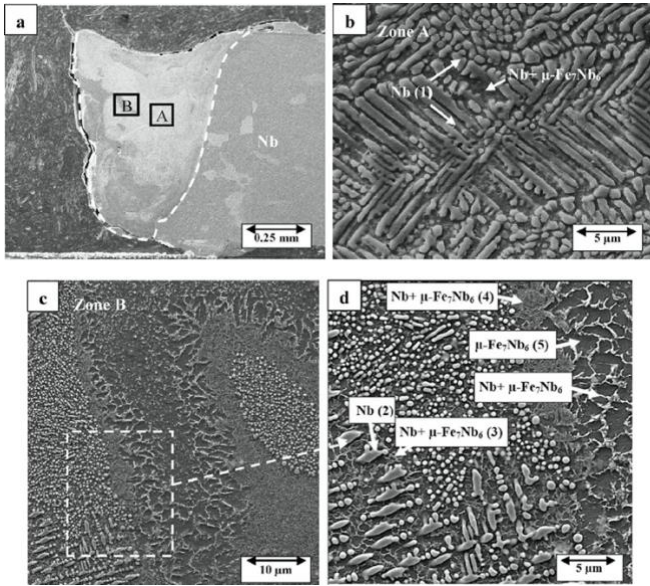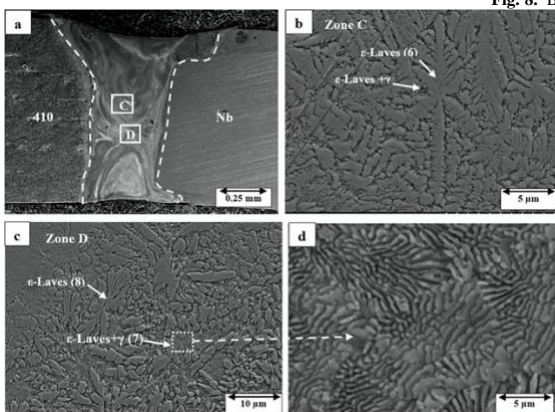
Fig. 7. Microstructure of Niobium to 410 stainless steel dissimilar laser weld without ESD interlayer, a. Low magnification, b. High magnification of zone A, c. High magnification of zone B, d. Higher magnification of illustrated part of zone B.
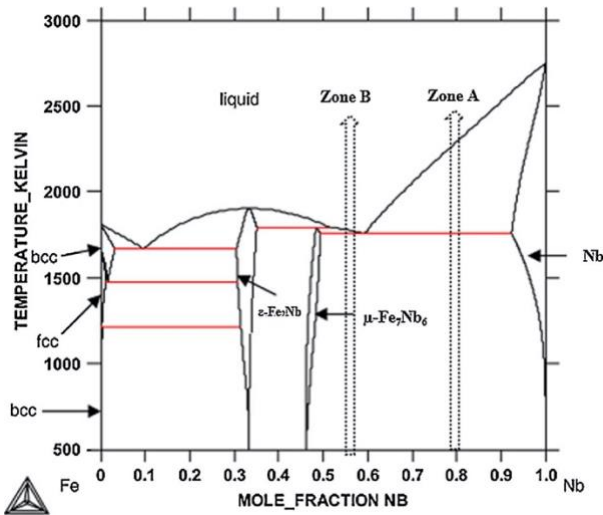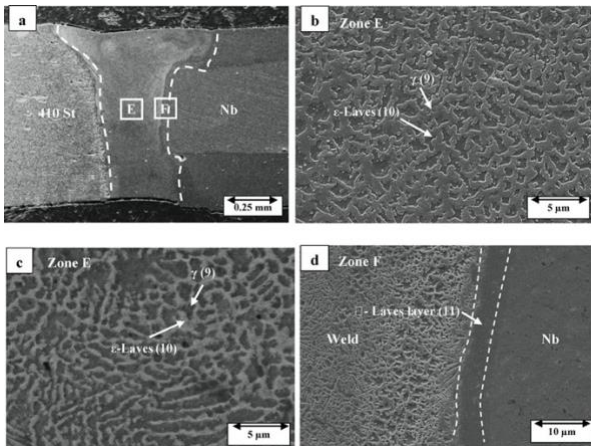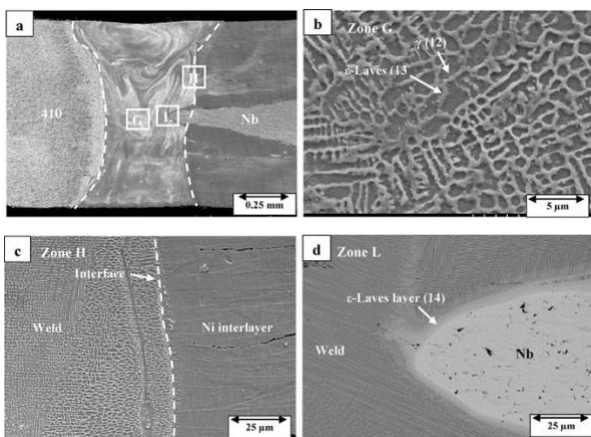

Fig. 8. Binary phase diagram of Fe/Nb [10].

Fig. 9. Microstructure of Nb to 410 stainless steel dissimilar laser weld with 0.25 mm nominal thickness ESD interlayer, a. Low magnification of weld zone, b. High magnification of zone C, c. High magnification of zone D, d. Higher magnification of fully eutectic -Laves + phases in zone E.

Fig. 10. Microstructure of Nb to 410 stainless steel dissimilar laser weld with 0.5 mm nominal thickness ESD interlayer, a. low magnification of weld zone, b. high magnification of zone E, c. backscatter image of zone E, d. high magnification of zone F.

Fig. 11. Microstructure of Nb to 410 stainless steel dissimilar laser weld with 1 mm nominal thickness ESD interlayer, a. low magnification of weld zone, b. high magnification of zone G, c. high magnification of zone H, d. high magnification of zone L.
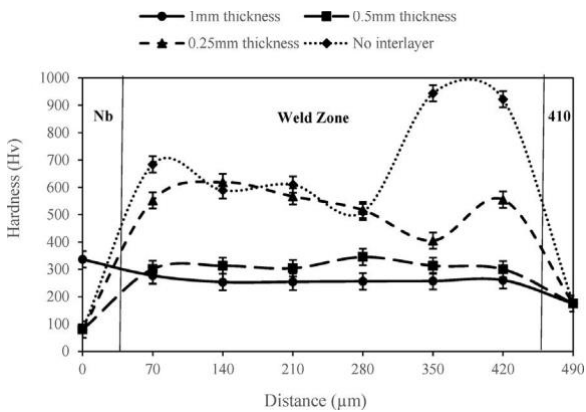
Fig. 12. Hardness profile of dissimilar laser weld of Nb to 410 stainless steel as a function of the ESD interlayer nominal thickness.
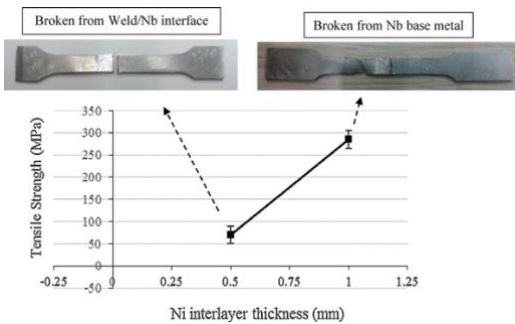
Fig. 13. Tensile test of dissimilar welded Nb to 410 stainless steel with 0.5 and 1 mm ESD interlayer thicknesses; a- showing 1 mm thick sample broken from Nb side and has high tensile strength and 0.5 mm thick sample broken from weld/Nb interface and has low tensile strength.

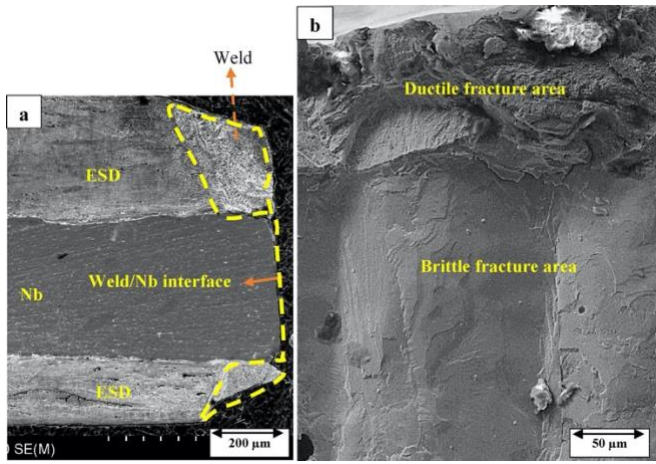**Fig. 14.** Fractography images of 0.5 mm interlayer thickness weld, a- cross section of fracture path, b- fracture surface morphology.